 DOI: 10.1002/masy.200950112

Effect of Chain Transfer Agents on Kinetics and Morphology of Poly(vinylidene fluoride) Synthesized in Supercritical Carbon Dioxide

*Muhammad Imran-ul-haq, Sabine Beuermann**

Summary: Vinylidene fluoride radical polymerizations were carried out using chain transfer agents of the general structure $C_6F_{13}X$, with X being I, Br or H. Homogeneity and monomer conversions were monitored by in-line spectroscopy. Apparent chain transfer constants at 120 °C are $8 \cdot 10^{-1}$, $8 \cdot 10^{-2}$ and $2 \cdot 10^{-4}$ for $C_6F_{13}I$, $C_6F_{13}Br$ and $C_6F_{13}H$, respectively, which may be associated to the C-X bond energy. The polymer end groups significantly influence the crystallinity of the polymer and the thermal stability.

Keywords: chain transfer agents; polymerization kinetics; supercritical CO_2; vinylidene fluoride

Introduction

Fluoropolymers in general exhibit high chemical inertness and thermostability, excellent hydro- and lipophobicity and valuable electrical properties. In addition, they may be characterized by low refractive indices, friction coefficients and relative permittivities. The polymers are non-sticky as well as resistant to UV, ageing, and to concentrated mineral acids and alkalis. Hence, their fields of applications are numerous.[1–6] Homo- and copolymers of vinylidene fluoride are particularly interesting, because they also exhibit excellent piezo- and pyroelectric properties.[7]

Vinylidene fluoride (VDF) polymers are usually produced in emulsion polymerizations employing fluorinated stabilizers. As a promising alternate reaction medium supercritical carbon dioxide is of high interest. In addition to being environmentally benign, carbon dioxide (CO_2) is non-toxic, non-flammable, inexpensive, volatile and readily available. It may easily be separated from polymers and the critical point is easily reached (critical temperature 31.1 °C; critical pressure 73.8 bar).[8] Moreover, rather high solubility of fluoropolymers in CO_2 was reported.[9] All these aspects render CO_2 an excellent reaction medium for polymerizations of fluorinated monomers.[10] DeSimone et al. first described homogeneous phase radical polymerization of fluoromonomers in $scCO_2$.[11] In case of VDF polymerizations, leading to semi-crystalline polymers, heterogeneous phase reactions in $scCO_2$ were reported.[12–16] Only recently, VDF polymerizations carried out in solution with $scCO_2$ were described.[17,18]

Fluorinated polymers of rather low molecular weight, so-called telogens, are of high technical importance, thus, the applicability of a large number of chain-transfer agents (CTAs) to radical polymerizations of fluorinated monomers was investigated.[5] For example, Ameduri et al. studied the influence of a variety of CTAs for polymerizations in acetonitrile in detail.[19] So far information on the use of CTAs for polymerizations in CO_2 is scarce. With respect to polymer properties and to phase behavior the use of highly fluorinated CTAs with the general structure

Institute of Chemistry, University of Potsdam, Karl-Liebknecht Str. 24-25, D 14476 Golm/Potsdam, Germany
E-mail: sabine.beuermann@uni-potsdam.de

of $C_6F_{13}X$ seems particularly attractive for VDF polymerizations in $scCO_2$. The perfluorinated hexyl group should not only lead to high thermal stability, in addition, it is expectedd to promote homogeneous phase reactions. In this publication three CTAs with X being l, Br or H are discussed. The formation of polymeric species containing halogen (I, Br) end-groups seems particularly interesting, because they may not only open the door for the introduction of other functionalities, these macromolecular species may have the potential to be used as macroinitiators in atom transfer radical polymerizations, which may enable the synthesis of block copolymers.[20–23]

This present work focuses on homogeneous phase VDF polymerization in $scCO_2$. Kinetic aspects as well as the influence of the CTAs on polymer morphology and thermal stability are discussed.

Experimental Part

Chemicals

All reactions were carried out with the monomer vinylidene fluoride (Solvay Solexis), carbon dioxide (grade 4.5, Messer Griesheim), and di-*tert*-butyl peroxide (DTBP, Akzo Nobel) as initiator. Polymer molecular weights were controlled by the chain-transfer agents perfluorinated hexyl iodide ($C_6F_{13}I$), perfluorinated hexyl bromide ($C_6F_{13}Br$) and 1H-perfluorohexane ($C_6F_{13}H$) provided by Dyneon. All chemicals were used as received.

Polymerizations

All VDF polymerizations in solution with 73 wt.% CO_2 were carried out at 1500 bar as detailed in our previous publications.[17,18] For polymerizations with 0.061 $mol \cdot L^{-1}$ DTBP and various amounts of $C_6F_{13}X$ the temperature was 120 °C, whereas PVDF with DTBP-derived end groups and $M_n = 3000$ $g \cdot mol^{-1}$ was obtained at 140 °C with 0.23 $mol \cdot L^{-1}$ DTBP in the absence of any CTA. The polymers were characterized as detailed below.

Characterization

Molecular weight distributions (MWDs) were obtained via size-exclusion chromatography with N,N–dimethylacetamide (DMAc, 99%, Acros, Germany) containing 0.1% LiBr (99% Riedel deHaen, Germany) as eluent and a column temperature of 45 °C. The set-up consists of an Agilent 1200 isocratic pump, an Agilent 1200 refractive index detector, and two GRAM columns (10 μm, 8x300mm, pore sizes 100 and 1000) from Polymer Standards Services (PSS). Polystyrene standards (PSS) were used for calibration.[17] ^{1}H-NMR spectra of PVDF dissolved in acetone-d_6 were recorded on a Bruker 300 MHz spectrometer to determine polymer end groups. To obtain information on the morphology, the samples were analyzed with a Field Emission Scanning Electron Microscope (Hitachi S-4800) at accelerating voltage of 2.0 kV. Thermogravimetric analyses (TGA) were performed under nitrogen atmosphere from 30 to 800 °C at a heating rate of 10 °C/min using a Linseis L81 thermal analyzer (Linseis, Germany) working in the vertical mode. Al_2O_3 was used as reference.

Results and Discussion

Polymerizations

VDF polymerizations with 73 wt. % CO_2 were carried out using the above-mentioned CTAs. The initiator concentration was 0.061 $mol \cdot L^{-1}$ and the chain transfer agent concentrations as detailed in Table 1. In addition, Table 1 contains number average molecular weights, M_n, polydispersities, *PDI*, and states whether the reaction mixture was homogeneous or heterogeneous. With the exception of the first entry in Table 1, monomer conversions were always higher than 90%. It should be noted that *heterogeneous* refers to the occurrence of two phases. Precipitation of polymer was not observed. The data in Table 1 and in Figure 1 indicate that the strongest chain transfer activity occurs with $C_6F_{13}I$. For example, a CTA concentration of

Table 1.
Molecular weight and conversion data obtained from VDF polymerizations in 73 wt.% CO_2 at 120 °C and 1500 bar with 0.061 mol · L^{-1} DTBP. The data for $C_6F_{13}I$ were taken rom ref. [38].

CTA	[CTA]/mol · L^{-1}	M_n/(g · mol^{-1})	*PDI*	Phase
$C_6F_{13}I$	0.07[a)]	3000	1.3	Homogeneous
$C_6F_{13}I$	0.03	8100	1.7	Homogeneous
$C_6F_{13}I$	0.05	6700	1.5	Homogeneous
$C_6F_{13}I$	0.10	3900	1.5	Homogeneous
$C_6F_{13}I$	0.15	3500	1.4	Homogeneous
$C_6F_{13}I$	0.20	1800	1.2	Homogeneous
$C_6F_{13}I$	0.25	1600	1.2	Homogeneous
$C_6F_{13}Br$	0.05	16900	3.0	Heterogeneous[b)]
$C_6F_{13}Br$	0.11	11900	4.3	Heterogeneous[b)]
$C_6F_{13}Br$	0.22	8800	2.9	Heterogeneous[b)]
$C_6F_{13}Br$	0.46	5600	2.2	Heterogeneous[b,c)]
$C_6F_{13}H$	0.05	32100	3.7	Heterogeneous[b)]
$C_6F_{13}H$	0.22	34200	2.1	Heterogeneous[b)]
$C_6F_{13}H$	0.44	32500	2.4	Heterogeneous[b)]

[a)]no initiator, 30% conversion; [b)]the reaction mixture shows two phases, precipitation does not occur; [c)]homogeneous up to 20% VDF conversion.

0.2 mol · L^{-1} leads to polymer with $M_n = 1800$ g · mol^{-1} in case of $C_6F_{13}I$, whereas M_n values of 8800 and 34200 g · mol^{-1} were obtained with $C_6F_{13}Br$ and $C_6F_{13}H$, respectively. Moreover, for the iodo and bromo compound the expected variation of M_n with CTA concentration is observed. In contrast, an increase in $C_6F_{13}H$ concentration did not cause any lowering of M_n. Some chain transfer activity is anticipated, since polydispersities are slightly lower at higher CTA concentration. However, no obvious trend is observed, which may also be due to the rather poor mixing of the system (no active stirring in the high-pressure cell).

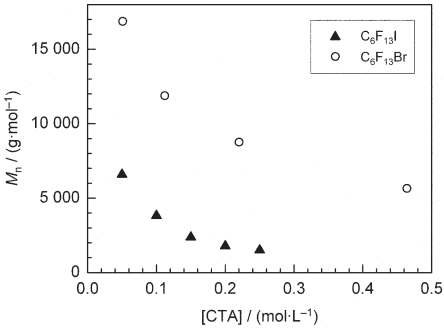

Figure 1.
M_n as a function of CTA concentration for PVDF from polymerizations at 120 °C and 1500 bar with 73 wt. % CO_2 using PFHI and PFBH as CTAs.

The data in Table 1 also shows that $C_6F_{13}I$ positively affects the homogeneity in the polymerization mixture. All VDF polymerizations in the presence of $C_6F_{13}I$ led to very high conversion in homogeneous phase. In contrast, the use of the bromo compound resulted in polymerization mixtures showing two phases. Only at the highest concentration of $C_6F_{13}Br$ and, thus, the lowest polymer molecular weight, the mixture remained homogeneous up to 20% conversion before turning heterogeneous.

Polydispersity values around 1.2 as obtained for the use of $C_6F_{13}I$ are indicative of a living radical polymerization systems.[24] Previously, employing ^{1}H-NMR and electrospray ionization mass spectrometry it was shown that the polymer exclusively contains $C_6F_{13}I$-derived end groups, while end groups originating from the initiator were not seen.[25] The other two CTAs led to significantly higher polydispersityies between 2.2 and 3.7, which are indicative of a conventional free radical polymerization. To confirm the interpretation of the molecular weight data ^{1}H-NMR spectra of PVDF samples obtained in the presence of $C_6F_{13}Br$ and $C_6F_{13}H$ were measured to determine the polymer end groups. The spectra are given in Figure 2 and 3, respectively.

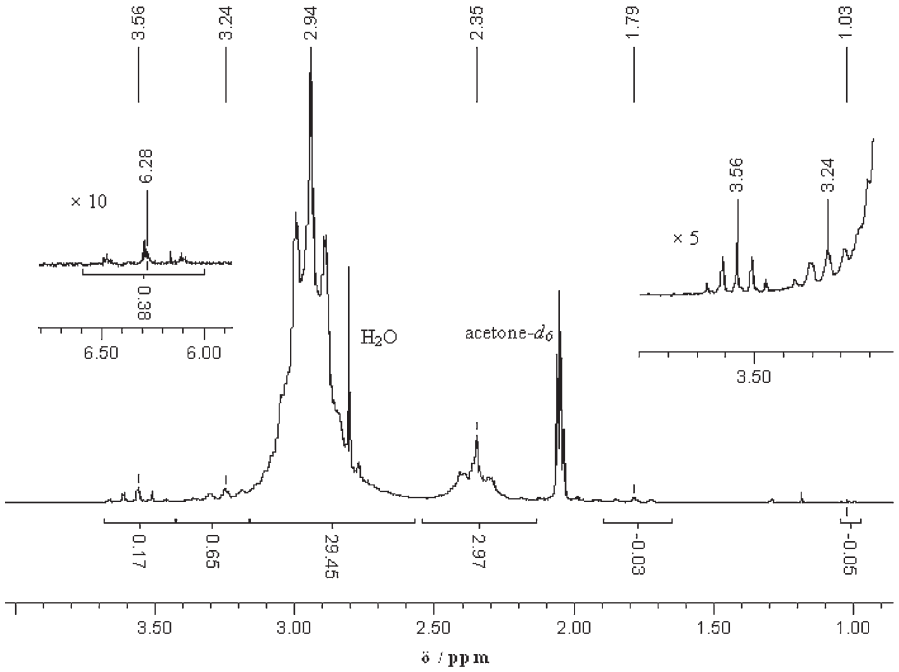

Figure 2.
^{1}H-NMR spectrum of polymer obtained from VDF polymerization using perfluorinated hexyl bromide (0.464 mol · L^{-1}) at 120 °C, 1500 bar with 73 wt. % CO_2. NMR solvent: acetone-d_6.

The ^{1}H-NMR spectrum in Figure 2 refers to PVDF from a reaction with $C_6F_{13}Br$. The following peaks may be assigned to the major structural units:[26]

-CF_2-***CH₂***-CH_2-CF_2-	multiplet, 2.35 ppm
–***CH₂***-CF_2–	multiplet, 2.94 ppm
C_6F_{13} – ***CH₂***–	triplet, 3.24 ppm
-***CH₂***-CF_2-Br	quintet, 3.56 ppm
H-*CF*$_2$-CH_2-	triplet of triplet,6.3 ppm

The signals at 2.06 and 2.81 ppm in the NMR spectra of Figure 2 and 3 refer to the solvent acetone and traces of water. Significant contributions from initiator-derived end groups are not seen in the spectrum in Figure 2. Signals of methyl protons from DTBP-derived end groups are expected to be found at 1.3 ppm in case of (***CH***$_3$)$_3$C–O– end groups, at 1.0 and 1.8 ppm in case of methyl protons in ***CH***$_3$–CH_2–CF_2- and ***CH***$_3$–CF_2–CH_2, respectively.[19] Thus, it may be concluded that chain transfer is the dominating chain initiating and chain stopping event in the presence of $C_6F_{13}Br$.

The ^{1}H-NMR spectrum in Figure 3, referring to polymerizations with $C_6F_{13}H$, indicates that C_6F_{13}–***CH₂***– end groups that should result in a triplet at 3.24 ppm are not contained in the polymer. Moreover, $C_6F_{13}H$ should also result in –CH_2–CF_2–***H*** as end group associated with a distinct peak at 6.3 ppm.[27] However, even the tenfold magnification of the spectrum shows only a peak of negligible intensity at 6.3 ppm. The integral of the peak is mainly due to scattering of the baseline. Thus, it is concluded that $C_6F_{13}H$ does not undergo significant chain transfer. The peak at 1.02 ppm refers to the initiator derived end group ***CH***$_3$–CH_2–CF_2–. Additionally, the triplet seen around 1.79 ppm refers to ***CH***$_3$–CF_2–CH_2–. The intensity of the latter peak is higher, which may be explained by the favoured formation of the more stable CH_3–CH_2–CF_2 radical compared to

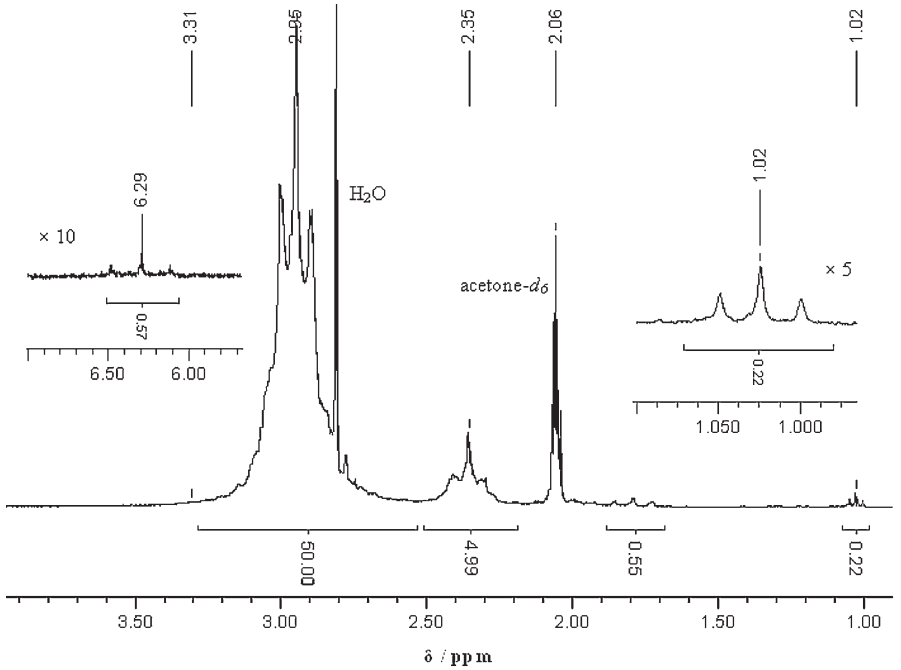

Figure 3.
^{1}H-NMR spectrum of polymer obtained from VDF polymerization using 1H-perfluorohexane (0.224 mol · L^{-1}) at 120 °C, 1500 bar with 73 wt. % CO_2. NMR solvent: acetone-d_6.

a CH_3–CF_2–CH_2 radical upon addition of a methyl radical to a monomer unit.

According to the work of Ameduri et al., e.g. ref. 19, ^{1}H-NMR spectra also give access to the fraction of defect structures that were formed by addition of a radical to the CF_2-side of the monomer rather than to CH_2, which would yield the more stable radical. From Figure 2 and 3 the fraction of defect structures is calculated to be 8%, which is close to the value of 7% derived for PVDF with $C_6F_{13}I$-derived end groups.[26] Thus, the fraction of defect structures is independent of how molecular weights are controlled. As indicated by the low intensities of the ^{1}H-NMR peaks at 6.3 in Figure 2 and 3 the contributions from chain transfer of H, e.g., via transfer to polymer, are minor.

To quantify the chain transfer activity of the three CTAs the chain transfer constants were determined from a Mayo plot[28,29] of $1/DP_n$ vs. [CTA]/[VDF], with $DP_n = M_n/M_{VDF}$ and the concentrations of CTA, [CTA], and VDF, [VDF]. Since the Mayo method was derived for low monomer conversions, and since with $C_6F_{13}Br$ and $C_6F_{13}H$ two phases occurred, the reported chain transfer constants, C_T^{app}, are considered as apparent. Nevertheless, they allow for a comparison of the overall transfer performance. Data for all three systems is given in Figure 4. The data points obtained

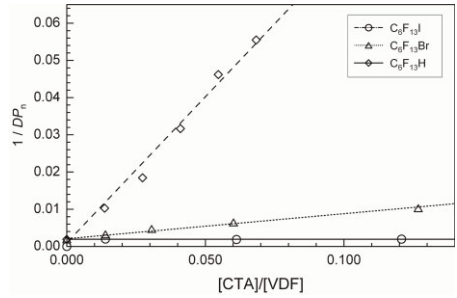

Figure 4.
DP_n^{-1} as a function of [CTA]/[VDF] for VDF polymerizations at 120 °C and 1500 bar in the presence of $C_6F_{13}I$, $C_6F_{13}Br$ and $C_6F_{13}H$.

for polymerizations in the presence of $C_6F_{13}H$ are independent of the $C_6F_{13}H$ concentration and may serve as limiting value for transfer in systems without any CTA. The C_T^{app} values derived from the slopes of the linear fits for the other two systems show that perfluorinated hexyl iodide is the most efficient chain transfer agent, represented by $C_T^{app} = 8 \cdot 10^{-1}$. For comparison the C_T^{app} value for $C_6F_{13}Br$ is one order of magnitude lower: $C_T^{app} = 8 \cdot 10^{-2}$. For $C_6F_{13}H$ a very low C_T^{app} of $2 \cdot 10^{-4}$ was determined, which is 1.5 and 3.5 orders of magnitude lower than the value for the bromine and iodine compound, respectively. The reason for the high C_T^{app} value for perfluorinated hexyl iodide may be seen in the low dissociation energy of the C-I bond compared to the C-Br and C-H bond. The bond dissociation energies (*BDE*) increase as follows:[30]

$$BDE(\mathrm{C-I}) = 213\ \mathrm{kJ \cdot mol^{-1}} < BDE(\mathrm{C-Br}) = 284\ \mathrm{kJ \cdot mol^{-1}} < BDE(\mathrm{C-H}) = 414\ \mathrm{kJ \cdot mol^{-1}}$$

To study the influence of $C_6F_{13}X$ concentrations on the rates of polymerization, these rates were calculated from NIR spectra recorded during the polymerization.[17] The data analysis was restricted to 40% of conversion to limit the influence of decreasing pressure due to volume contraction caused by the differences in polymer and monomer density. For comparison, the rates of polymerization, r_p, for VDF polymerizations with $C_6F_{13}I$, $C_6F_{13}Br$ and $C_6F_{13}H$ are depicted in Figure 5a. For $C_6F_{13}I$ a clear increase in rate with higher CTA concentration is found. Even at the lower $C_6F_{13}I$ concentration r_p is significantly higher than for the two other CTAs. The chain length dependence of the termination rate coefficient, k_t, should not be responsible for the observed variation in r_p: with increasing CTA concentration the chain lengths are reduced and k_t will increase leading to a slower rate of polymerization. In contrast, an increase in r_p with $C_6F_{13}I$ concentration was observed experimentally. A possible explanation may be seen in contributions of $C_6F_{13}I$ to the initiation reaction. The first entry in Table 1 indicates that VDF polymerizations in the absence of DTBP may be carried out, if $C_6F_{13}I$ is present. Experiments without $C_6F_{13}I$ and DTBP did not yield any polymer.

In contrast, the rate data for polymerizations with $C_6F_{13}H$ and for the lower concentration of $C_6F_{13}Br$ are the same within experimental certainty. Still, for $C_6F_{13}Br$ the unexpected increase in r_p with

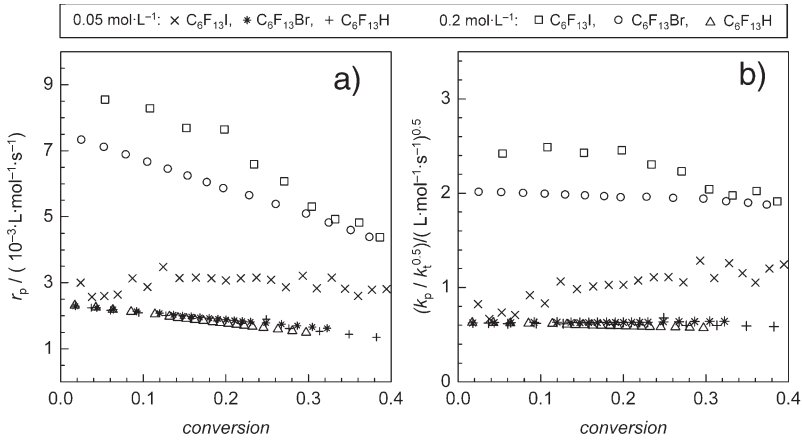

Figure 5.
r_p - conversion (left) and $k_p/k_t^{0.5}$ - conversion (right) plots for VDF polymerization at 120 °C, 1500 bar with 73 wt. % CO_2, 0.061 mol · L^{-1} DTBP, 3.66 mol · L^{-1} VDF with CTA concentrations as indicated.

higher amounts of CTA is noticeable. The enhanced reaction rates are surprising since the molecular weight data indicate not only a much weaker chain transfer activity, but also that living conditions are not established (high PDI), which are in line with the higher *BDE* of C–Br bonds. If the C–Br bond affords more energy to be cleaved, it was anticipated that $C_6F_{13}Br$ does not contribute significantly to initiation. The rate data suggest, however, that there is some contribution of $C_6F_{13}Br$ on the rate.

According to $r_p = (f \cdot k_d \cdot c_I \cdot k_t^{-1})^{0.5} \cdot k_p \cdot c_{VDF}$, with the propagation rate coefficient, k_p, initiator decomposition rate coefficient, k_d, efficiency, f, VDF concentration, c_{VDF}, and initiator concentration, c_I, the coupled parameter $k_p/k_t^{0.5}$ may be calculated. Using $k_d = 6.4 \cdot 10^{-6}$ s^{-1} and $f = 1$ estimated as detailed in ref. 18, $k_p/k_t^{0.5}$ values depicted in Figure 5b were derived, which naturally show a similar behaviour as the corresponding rate data: $k_p/k_t^{0.5}$ values are identical for the lower $C_6F_{13}Br$ and both $C_6F_{13}H$ concentrations, whereas the experiments with $C_6F_{13}I$ or 0.2 $mol \cdot L^{-1}$ $C_6F_{13}Br$ yield significantly higher values. In all cases a rather weak variation of $k_p/k_t^{0.5}$ with conversion is observed. This finding is not surprising due to the rather low VDF concentrations and low molecular weights.

Due to the above-discussed contributions of $C_6F_{13}I$ and to a lesser extent of $C_6F_{13}Br$ on initiation the rate data for these systems are not considered for further kinetic analyses. The finding that $C_6F_{13}H$ concentration does not affect r_p suggests that no side reactions were induced. Thus, it may be concluded that reliable values for $k_p/k_t^{0.5}$ were determined. To obtain a rough estimate for the individual rate coefficients k_p and k_t the following approach was applied: Since termination is a diffusion controlled reaction, it was assumed that k_t of the structural similar ethene should provide a reasonable estimate for k_t of VDF. Using a k_t value of $9.6 \cdot 10^7$ $L \cdot mol^{-1} \cdot s^{-1}$ calculated for ethene at 120 °C and 1500 bar according to ref. [31], apparent k_p values were estimated. For polymerization in the presence of $C_6F_{13}H$ k_p in the order of $6 \cdot 10^3$ $L \cdot mol^{-1} \cdot s^{-1}$ is obtained. This value is by a factor of 3 higher than the corresponding ethene value at identical conditions. An increase in k_p in going from ethene to VDF seems reasonable, since the double bond is expected to be more reactive towards radical addition due to the electron withdrawing fluorine atoms as substituents. To test whether these estimates are reliable and to decouple k_p and k_t, pulsed laser initiated polymerizations should be carried out in the future.[32]

Morphology of PVDF

Visual observation of the PVDF samples indicated that different morphologies ranging from fine free-flowing powder to coagulated materials were found. To get further information on the morphology, SEM images were considered. As an example, Figure 6 gives the images for PVDF with $M_n \sim 6000$ $g \cdot mol^{-1}$ obtained from reactions with $C_6F_{13}I$ and $C_6F_{13}Br$. The SEM image for sample $C_6F_{13}Br$ shows coagulated material with some irregular voids. SEM images of PVDF with $C_6F_{13}I$-derived end groups results in more regular material that shows small structures in the range of 10 μm. Magnification shows lamellae-type structures with fine voids. The observation of these different morphologies is in accordance with the visual impression of the polymers.

Since the morphology of PVDF samples with different end groups differs significantly, it seemed rewarding to analyze the polymers with respect to degree of crystallinity and the crystal phases present in the material. PVDF is known to occur in five different crystalline phases, which are distinguished by the conformation of the C–C bonds along the polymer main chain.[33] The crystalline phases may be distinguished by differences in their IR spectra.[34–37] As an example, α phase material gives rise to a peak at 795 cm^{-1} and β phase material to a peak at 840 cm^{-1}. Previously, the latter assignment was confirmed by wide angle X-ray scattering and it was shown that PVDF with $C_6F_{13}I$-derived end groups shows the lowest content of

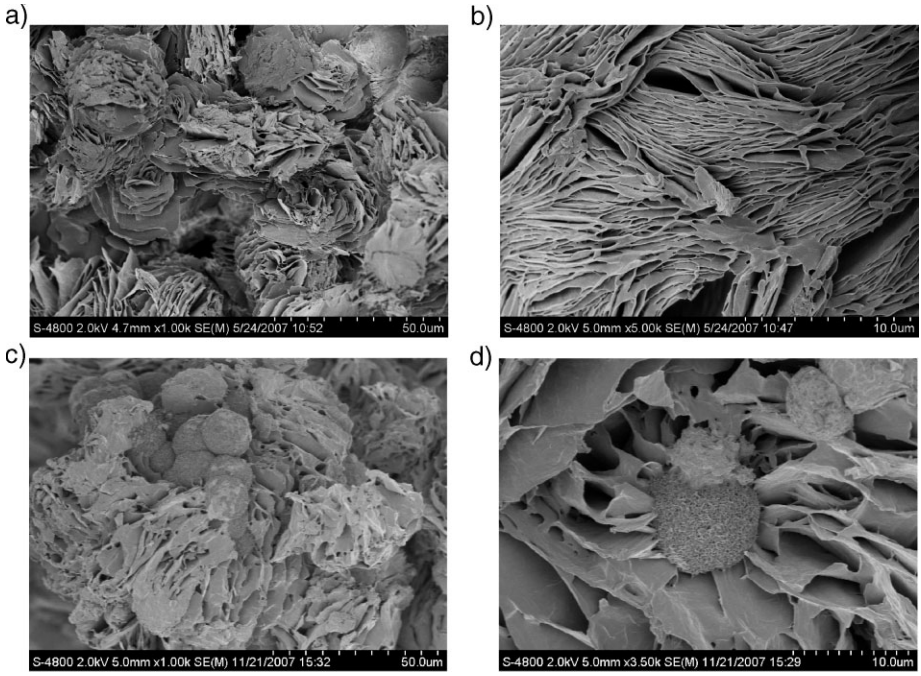

Figure 6.
Scanning electron microscopy images of PVDF samples with $M_n \sim 6000\ g \cdot mol^{-1}$ and end groups originating from $C_6F_{13}I$ (a,b), and $C_6F_{13}Br$ (c,d) collected after expansion of the reaction mixture to ambient conditions.

β phase material compared to PVDF with methyl or $BrCCl_3$-derived end groups.[26] The overall degree of crystallinity determined via differential scanning calorimetry (DSC) was highest for PVDF with $C_6F_{13}I$- and lowest for DTBP-derived end groups. Comparison of IR spectra for PVDF with $C_6F_{13}I$ and $C_6F_{13}Br$-derived end groups indicates that the fraction of β phase material is higher for the bromine end group. DSC analyses revealed that the overall degree of crystallinity is around 60% for polymers with M_n between 2400 and 8100 $g \cdot mol^{-1}$ for $C_6F_{13}I$-derived end groups. A lowering of crystallinity to 52% was obtained for PVDF with $C_6F_{13}Br$-derived end groups and $M_n = 6000\ g \cdot mol^{-1}$. Since the polymers are only different with respect to the halogen end group, the results indicate that these halogen atoms significantly contribute to the degree of crystallinity and to the type of crystal phase formed: The larger the halogen atom, the higher the degree of crystallinity, however, the lower the fraction of β phase material. Because PDI values are slightly different, in future experiments the impact of PDI should also be investigated.

Thermal Stability

Thermogravimetric analyses (TGA) were carried out to study the influence of polymer end groups on the thermal stability of

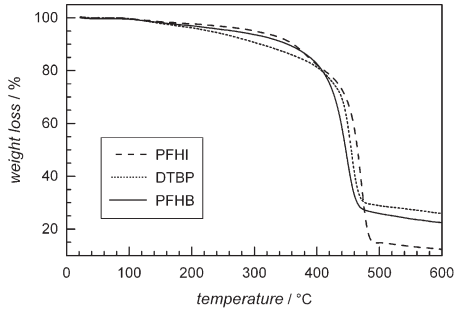

Figure 7.
Thermogravimetric analysis of PVDF with end groups derived from $C_6F_{13}I$, $C_6F_{13}Br$ and DTBP at 20 °C/min under nitrogen.

Table 2.
Residual polymer weight fractions, w_p, observed at 200, 300 and 450 °C.

sample	end groups	M_n/g · moL^{-1}	*PDI*	w_p (T_{200})	w_p (T_{300})	w_p (T_{450})
PFHI	C_6F_{13}, I	3305[a)]	1.5	97.7	94.9	67.5
PFHB	C_6F_{13}, Br	3450[b)]	2.3	97.0	93.8	49.0
DTBP	CH3	3031[c)]	4.0	96.2	90.8	60.9

Molecular weight control via
[a)]0.10 mol · L^{-1} $C_6F_{13}I$; [b)]0.92 mol · L^{-1} $C_6F_{13}Br$; [c)]0.23 mol · L^{-1} DTBP.

the polymers. The analyses were carried out for polymers with M_n between 3000 and 3500 g · mol^{-1}. The end groups originate from the CTAs $C_6F_{13}I$ and $C_6F_{13}Br$ and from the initiator DTBP. The TGA curves are depicted in Figure 7 and the results are listed in Table 2.

The TGA curves in Figure 7 are rather similar, despite the different end groups. The first significant weight loss of approximately 3% is observed at about 200 °C and is due to evaporation of water. An increase in temperature to 300 °C leads to an additional slight decrease in mass up to a total loss of 5 to 9%. The highest thermal stability with a weight loss of 5% at 300 °C for sample PFHI with $C_6F_{13}I$-derived end groups may be assigned to the comparably high degree of crystallinity of 60%. For PVDF with $C_6F_{13}Br$-derived (PFHB) or DTBP-derived end groups (DTBP) the weight loss at 300 °C amounts to 6 and 9%, respectively. These results are also in line with crystallinity data, since for DTBP-derived end groups the crystallinity is below 30%,[26] whereas bromine containing CTA results in polymer with 52% of crystallinity. In view of the large variations in crystallinity the differences in TGA curves seem rather small. This finding may be due to the fact that the melting temperatures for all samples are well below 200 °C. Thus, all samples are already in the molten state when differences in the TGA curves start to occur.

Conclusion

Homogeneous phase VDF polymerizations in $scCO_2$ were carried out with CTAs of the general type $C_6F_{13}X$. The apparent chain transfer constants, C_T^{app}, are $8 \cdot 10^{-1}$, $8 \cdot 10^{-2}$ and $2 \cdot 10^{-4}$ for $C_6F_{13}I$, $C_6F_{13}Br$ and $C_6F_{13}H$, respectively. The strong dependence of C_T^{app} on the X-atom in $C_6F_{13}X$ may be related to the bond dissociation energies of C-X: The stronger the C-X bond the lower C_T^{app}. The NMR analyses show insertion of VDF units between the two ends of the CTAs in case of $C_6F_{13}I$ and $C_6F_{13}Br$. The fraction of DTBP-derived end groups is negligible. $k_p/k_t^{0.5}$ was estimated to be 0.65 $(L \cdot mol^{-1} \cdot s^{-1})^{0.5}$ for VDF polymerizations at 120 °C and 1500 bar in solution with 73 wt.% CO_2.

The use of $C_6F_{13}I$ and $C_6F_{13}Br$ as CTAs for molecular weight control did not only result in polymer that shows higher thermal stability than corresponding polymers with DTBP-derived end groups. In addition, the polymers with halogen atoms as end groups may be attractive for subsequent functionalization.

Acknowledgements: The authors gratefully acknowledge financial support by *Dyneon*, *Germany*. We are grateful to Dr. Brigitte Tiersch for SEM analysis and to Dr. Alwin Friedrich for TGA measurements. Additional support by the Deutsche Forschungsgemeinschaft within the European Graduate School ''Microstructural Control in Radical Polymeriazation'' is acknowledged.

[1] B. Boutevin, Y. Pietrasanta, *Les Acrylates et Polyacrylates Fluore's*, Erec, Paris **1989**.
[2] J. Scheirs, *Modern Fluoropolymers: High Performance Polymers for Diverse Applications*, Wiley, New York **1997**.
[3] G. Hougham, P. E. Cassidy, K. Johns, T. Davidson, Eds., *Fluoropolymers. 2. Properties*, Kluvert, New York **1999**.

[4] R. Bongiovanni, F. Montefusco, A. Priola, N. Macchioni, S. Lazzeri, L. Sozzi, B. Ameduri, *Prog. Org. Coat.* **2002**, *45*, 359.
[5] B. Ameduri, B. Boutevin, *Well-Architectured Fluoropolymers: Synthesis,Properties and Applications*, Elsevier, Amsterdam **2004**.
[6] W. E. Hanford, R. M. Joyce, Jr., US Patent 2,440, 800 (**1948**).
[7] Z.-M. Dang, Y.-H. Lin, C.-W. Nan, *Adv. Mater.* **2003**, *15*, 1625.
[8] P. G. Jessop, W. Leitner, Eds., *Chemical Synthesis Using Supercritical Fluids*, Wiley-VCH, Weinheim **1999**.
[9] C. F. Kirby, M. A. McHugh, *Chem. Rev.* **1999**, *99*, 565.
[10] J. L. Kendall, D. A. Canelas, J. L. Young, D. M. DeSimone, *Chem. Rev.* **1999**, *99*, 543.
[11] J. M. Desimone, Z. Guan, C. S. Elsbernd, *Science* **1992**, *257*, 945.
[12] P. A. Charpentier, J. M. DeSimone, G. W. Roberts, *Ind. Eng. Chem. Res.* **2000**, *39*, 4588.
[13] M. K. Saraf, S. Gerard, L. M. Wojcinshi, II, P. A. Charpentier, J. M. DeSimone, G. W. Roberts, *Macromolecules* **2002**, *35*, 7976.
[14] P. A. Mueller, G. Storti, M. Morbidelli, I. Costa, A. Galia, O. Scialdone, G. Filardo, *Macromolecules* **2006**, *39*, 6483.
[15] H. Tai, W. Wang, R. Martin, J. Liu, E. Lester, P. Licence, H. M. Woods, S. M. Howdle, *Macromolecules* **2005**, *38*, 355.
[16] U. Beginn, R. Najjar, J. Ellmann, R. Vinokur, R. Martin, M. Moeller, *J. Poly. Sci., Part A: Polym. Chem.* **2006**, *44*, 1299.
[17] S. Beuermann, M. Imran ul-haq, *J. Polym. Sci., Part A: Polym Chem.* **2007**, *45*, 5626.
[18] S. Beuermann, M. Imran ul-haq, *Macromol. Symp.* **2007**, *259*, 210.
[19] M. Duc, B. Ameduri, G. David, B. Boutevin, *J. Fluorine Chem.* **2007**, *128*, 144.
[20] M. Destarac, J. M. Bessiere, B. Boutevin, *Macromol. Rapid. Commun.* **1997**, *18*, 967.
[21] K. Matyjaszewski, J. Xia, *Chem. Rev.* **2001**, *101*, 2921.
[22] M. Destarac, K. Matyjaszewski, E. Silverman, B. Ameduri, B. Boutevin, *Macromolecules* **2000**, *33*, 4613.
[23] B. Ameduri, B. Boutevin, P. Gramain, *Adv. Polym. Sci.* **1997**, *127*, 87.
[24] M. Imran ul-haq, *PhD thesis*, Potsdam, **2008**.
[25] G. Moad, D. H. Solomon, *The Chemistry of Radical Polymerization*, 2nd ed., Elsevier, Amsterdam **2006**.
[26] M. Imran ul-haq, B. Tiersch, S. Beuermann, *Macromolecules* ASAP article, 4 October **2008**.
[27] M. Pianca, E. Barchiesi, G. Esposto, S. Radice, *J. Fluorine Chem.* **1999**, *95*, 71.
[28] C. Boyer, D. Valade, L. Sauguet, B. Ameduri, B. Boutevin, *Macromolecules* **2005**, *38*, 10353.
[29] F. R. Mayo, *J. Am. Chem. Soc.* **1943**, *65*, 2324.
[30] Approaches for living systems resting on measurements of VDF and CTA consumption could not be used, since $C_6F_{13}I$ concentration as a function of time was not accessible.
[31] http://www.cem.msu.edu/∼reusch/OrgPage/bndenrgy.html.
[32] M. Buback, J. Schweer, *Z. Phys. Chem. N. F.* **1989**, *161*, 153.
[33] S. Beuermann, M. Buback, *Prog. Polym. Sci.* **2002**, *27*, 191.
[34] S. L. Hsu, F. J. Lu, D. A. Waldman, M. Muthukumar, *Macromolecules* **1985**, *18*, 2583.
[35] K. Tashiro, M. Kobayashi, H. Tadokoro, *Macromolecules* **1981**, *14*, 1757.
[36] E. Benedetti, S. Catanorchi, A. D'Alessio, G. Moggi, P. Vergamini, M. Pracella, F. Ciardelli, *Polym. Int.* **1996**, *41*, 35.
[37] M. Benz, W. B. Euler, *J. Appl. Polym. Sci.* **2003**, *89*, 1093.
[38] Y. Peng, P. Wu, *Polymer* **2004**, *45*, 5295.

